Analysis and mitigation of the wind induced response of large span suspended roofs: the case of the new Braga Stadium

Nicola Cosentino [a], Massimo Majowiecki [b]

[a]Dept. DISTART - University of Bologna, Bologna
[b] Dept. DCA - IUAV University of Venice - Venice

ABSTRACT

Due to the geometric complexity, the flexibility which induce large displacement and the small inherent damping, several aspects have to be taken into account during the design stage of a suspended large span roof. The analysis of wind induced vibration requires, for instance, the evaluation of the pressure coefficients, the structural response analysis, the investigation of possible aeroelastic effects, etc, up to the design of additional energy dissipative system to reduce the vibrations themselves, if necessary. A particularly interesting application of recent techniques to study the cited problems has been made for the new Stadium built in Braga (Portugal) for the Euro 2004 Games. The main objective of this paper is to study the structural response and its mitigation whit relatively simple analysis tools which allow to control the numerical results without using heavy analysis software and without loosing in precision. The appropriate use of orthogonal decomposition techniques is very helpful at this scope. Another goal of the paper is to review the design process from a unitary point of view. In fact, in the Authors experience, the different problems are usually studied by different specialists and the interference between the various aspects is often lost.

SOMMARIO

La complessità geometrica, gli spostamenti indotti dalla loro alta flessibilità ed il modestissimo smorzamento intrinseco, aprono diverse problematiche nella progettazione di coperture sospese di grande luce. L'analisi delle vibrazioni indotte dall'azione del vento, ad esempio, richiede una adeguata valutazione dei coefficienti di pressione, l'analisi stocastica della risposta, lo studio di possibili effetti aeroelastici, ecc., fino allo studio di eventuali sistemi dissipativi esterni, qualora i movimenti calcolati risultassero non accettabili. Un'applicazione particolarmente interessante di recenti tecniche per lo studio di tali problemi ha riguardato il nuovo Stadio costruito a Braga (Portogallo) in occasione del campionato di calcio Euro 2004. Il principale scopo di questo lavoro è lo studio della risposta strutturale e della mitigazione della stessa con strumenti di analisi relativamente semplici che consentano il controllo dei risultati numerici senza l'uso di pesanti software e senza trascurare elementi significativi del calcolo. L'uso appropriato delle tecniche di decomposizione ortogonale risulta particolarmente efficace allo scopo. Un altro obiettivo dell'articolo è quello di rivedere il processo di progettazione strutturale da un punto di vista unitario. Infatti, nell'esperienza degli scriventi, i diversi problemi sono spesso affrontati da diversi specialisti e l'interazione tra le varie problematiche viene non di rado trascurata.

KEYWORDS: Suspended Roof; Wind loads; POD; Aeroelasticity; Sensibility analysis; Response control.

1. INTRODUCTION

In the following, the analysis and the mitigation of the wind induced response on the new Braga Stadium suspended roof will be presented. Different orthogonal decomposition techniques have been used during the different stages of the structural design. This allow to control the numerical

results without loosing important aspects of the stochastic problems. The scientific literature often reports the above cited techniques without considering their effective helpfulness in the structural design. In the paper, the structural design process is globally presented and the application will show the effectiveness of the different orthogonal decomposition techniques in studying specific problems.
The wind induced response analysis is firstly reported. Then, the main results of an aeroelastic experimental study are given. A sensibility analysis will show some important aspects to take into account in evaluating the structural reliability. Finally, since the wind induced vibrations were found to be quite large, the preliminary design of an additional damping system is shown. Fig. 1 shows a general view of the Stadium and a scheme of the roof indicating the references used below.

2. WIND INDUCED RESPONSE ANALYSIS

Wind pressures are derived from a wind tunnel study, on a rigid scaled model, carried out by the RWDI. Since the pressure time histories were simultaneously measured at different points, within the upper and the lower sides of the roof panels, the instantaneous pressure fields were available.
The orthogonal decomposition techniques have been adopted to simplify the pressure representation, and to reduce the computational effort. Following the simplified procedure suggested by Vickery, 1993, the structural response to wind actions has been determined by separately evaluating (1) the mean response, (2) the quasi-steady response and (3) the resonant response. The first term simply takes into account the mean pressure distributions. The second one is obtained by performing a classical covariance proper orthogonal decomposition (POD). The third one takes into account the dynamic amplification of a suitable number of structural vibration modes, each one of them being excited by the unsteady wind pressures.
The static responses and the modal parameters used in the above cited calculations have been evaluated by mean of a finite element model of the structure, implemented on the FE software STRAND. Cable and shell and beam finite elements have been used to model the suspension cables, the roof panels and the connectors respectively. Linear analyses have been performed, the geometric stiffness matrix corresponding to the equilibrium configuration under gravity loads.

2.1. Wind tunnel data

Wind tunnel results were provided in terms of pressure coefficient time history series. Pressures on the concrete roof panels were simultaneously measured at 200 points, distributed on both the upper and the lower surfaces. Details on pressure taps distribution were reported by RWDI, 2001. Time series were provided for 36 wind directions, 10° spaced. The pressure coefficients were referenced to the mean dynamic pressure measured at a height equivalent to 600m (full scale) during the wind tunnel tests. The Cp data were listed as individual Cp's (i.e., they provided the top and underside pressures separately). Approximately 12250 points of Cp data were provided for each pressure tap location.

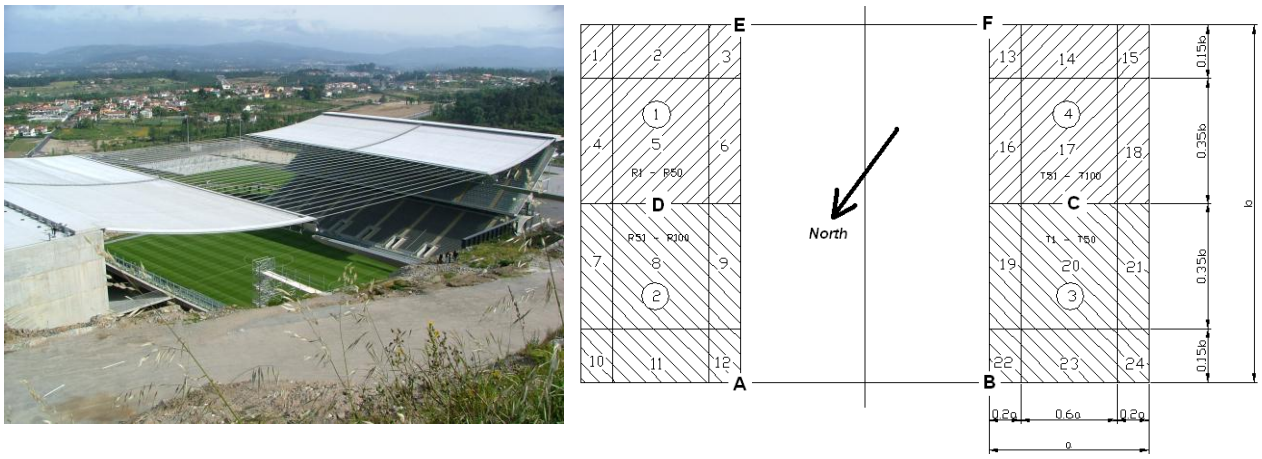

Figure 1. View of the Stadium from the south (a) and scheme of the roof (b).

Acquisitions were made at 512 samples per second for 24 seconds (corresponding to approximately 1 hour at full scale). The wind tunnel test speed at height equivalent to 600 m full scale was approximately 14.6 m/sec. Following the appropriate data scaling, from the model to the prototype scale (length scale L_s = 400, velocity scale V_s = 3.2, time scale T_s = 125), the measured pressures have been transformed in nodal (referred to the FEM model) values by mean of cubic spline interpolation.

2.2. General statistic features of pressure fields

In order to obtain the distribution of differential pressures main statistics, the unsteady pressure fields have been interpolated (cubic spline) and combined (upward and downward faces) for each record time instant. Differential pressure mean values, standard deviations, minima and maxima were evaluated for different incident wind directions. Mean values are used to evaluate the generic mean response (load, deflection, etc.) of the structure to wind actions. Standard deviations and extreme values are representative of local fluctuations and are used for local design evaluations. Fig. 2 reports the pressure coefficient mean values and standard deviations for a wind incidence of 270° from true north (the worst wind loading condition).

2.3. Classical covariance Proper Orthogonal Decomposition - POD

An unsteady multivariate pressure field can be usefully simplified by projecting (Proper Orthogonal Decomposition - POD) it on the space generated by the eigenvectors of the covariance matrix of the original field. Two main advantages can be achieved by this technique. Firstly, the new fields (pressure modes) are mutually uncorrelated, giving rise to advantages which will be explained in the next section. Secondly, the energy content of the complete multivariate field is usually well represented by few components in the transformed space, allowing the representation of the effective pressure field by mean of few pressure modes. A possible third advantage, which is still debated by the scientific community, consists in the physical correlation between pressure modes and aerodynamic phenomena (such as incident wind turbulence, vortex shedding, etc.). As a matter of fact, since the covariance is fully representative of the correlation only for Gaussian random processes, the pressure modes are mutually uncorrelated only for Gaussian multivariate pressure fields. It means that the POD method can usefully applied for global actions (were the non-Gaussianity becomes negligible) but not for the evaluation local loads.
Analytically, let $\boldsymbol{p}(t)=\{p_1(t) \ \dots \ p_m(t)\}^T$ be a Gaussian stationary nil mean m-variate random process. Let $\mathbf{C}_{\boldsymbol{p}}$ be the covariance (for $\tau = 0$) matrix of $\boldsymbol{p}(t)$. This matrix is symmetric and positive definite, thus it admits the modal decomposition:

$$\mathbf{C}_p = \sum_{k=1}^{m} \phi_k \phi_k^T \lambda_k \tag{1}$$

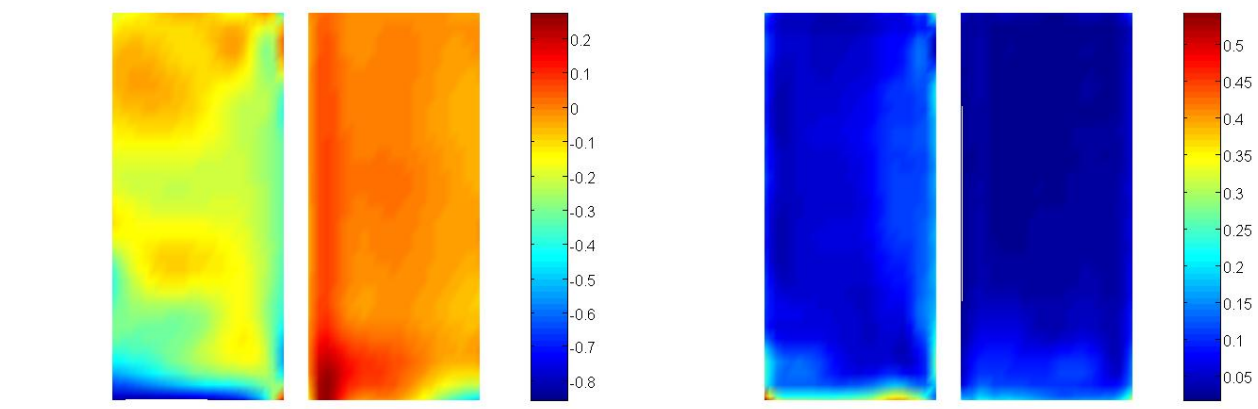

Figure 2. Pressure coefficient mean values (a) and standard deviations (b) for wind incidence 270° from true north.

where λ_k and ϕ_k are k^{th} eigenvalue and eigenvector of $\mathbf{C}_p$. The eigenvalues are real and positive; the eigenvectors follow the orthogonality properties:

$$\phi_i \phi_j^T = \delta_{ij}; \qquad \phi_i^T \mathbf{C}_p \phi_j = \delta_{ij} \lambda_j \; ; \qquad (i, j = 1, \ldots m) \tag{2}$$

where δ is the Kroneker's delta. By virtue of Eq. (2a), the eigenvectors of $\mathbf{C}_p$ constitute a base in the class of vectors with dimension m. The covariance transformation law is defined by:

$$\mathbf{p}(t) = \sum_{k=1}^{m} \phi_k x_k(t) \tag{3}$$

where $\boldsymbol{x}(t) = \{x_1(t) \ \ldots \ x_m(t)\}^T$ is the m-variate random process, image of $\boldsymbol{p}(t)$ in the transformed space. Furthermore, the Eq. (2b) shows that the covariance matrix $\mathbf{C}_x$ of $\boldsymbol{x}(t)$ is diagonal and its terms are the eigenvalues of $\mathbf{C}_p$. It means that, in the transformed space, $\boldsymbol{x}(t)$ is a vector of m uncorrelated (for $\tau = 0$) processes. By sorting the eigenvalues in decreasing order, Eqs. (1) and (2) may be cut off after a term of order s, suitably less than m.
Fig. 3 shows the eigenvectors ϕ_k and the eigenvalues λ_k (which represents the variance of the image field $x_k(t)$) for the firsts two pressure modes, for a wind incidence of 270° from north. Since the eigenvectors are steady quantities, the POD has been directly carried out on the measured pressure coefficients; then, the cubic spline interpolation has been applied to each eigenvector to obtain the nodal differential (upward and downward faces) values.

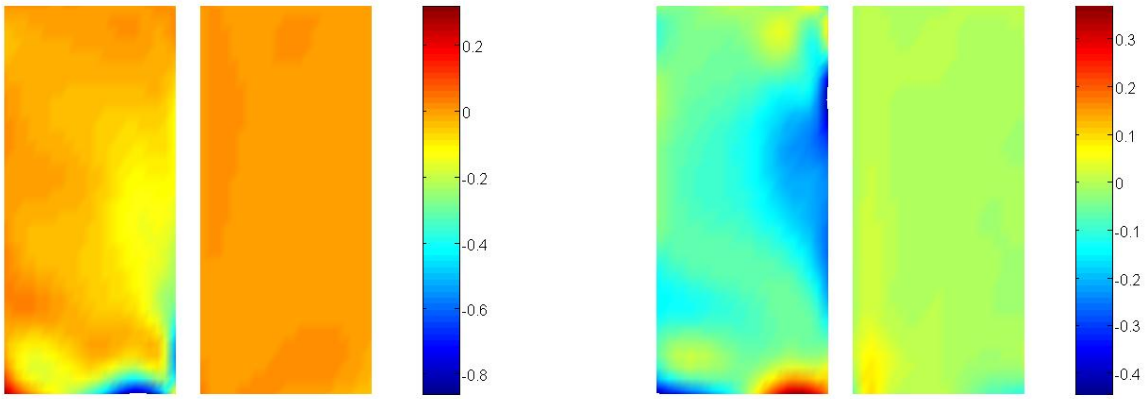

Figure 3. Cp modes (POD), wind 270° from true north: (a) Mode 1, $\sigma^2 = 0.1449$; (b) Mode 2 - $\sigma^2 = 0.0748$.

2.4. Quasi-steady effects

By virtue of Eq. (3) and after a cut off after a term of order s, the generic response $R(t)$ of a linear system to the load $\boldsymbol{p}(t)$ can be expressed as:

$$R(t) = \sum_{k=1}^{s} x_k(t) \cdot R_k \tag{4}$$

where R_k is the generic response (load, deflection, etc.) due to the static distribution ϕ_k. Thanks to the uncorrelation between $x_i(t)$ and $x_j(t)$ if $i \neq j$, the variance of the generic response, if resonant effects are neglected, is given by:

$$\sigma_{R,qs}^2 = \sum_{k=1}^{s} \sigma_{x_k}^2 R_k^2 \tag{5}$$

Finally, the quasi-steady peak (minimum and maximum) response can be obtained as:

$$R_{qs} = \overline{R} \pm g_{qs}\sigma_{R,qs}; \qquad \sigma_{R,qs} = \sqrt{\sigma^2_{R,qs}} \tag{6}$$

g_{qs} being the quasi-steady gust factor. For the case study of Braga Stadium, 38 pressure modes have been considered. The gust factor g_{qs} has been assumed to be 3.6 for each pressure mode. In Tab. 1, the mean, quasi-steady and resonant effects (see below) are compared, for the 270° from north wind direction, in terms vertical displacements (positive upward) of 6 significant roof points (as indicated in Fig. 1b).

2.5. Resonant effects

The resonant effects can be evaluated by using the relationship:

$$R_{qs+res} = \overline{R} \pm \sqrt{g^2_{qs}\sigma^2_{R,qs} + g^2_{res}\sigma^2_{R,res}}; \qquad g^2_{res}\sigma^2_{R,res} = \sum_{h=1}^{n} g^2_h \sigma^2_{R_h} \tag{7}$$

In Eq. (7b), n is the number of structural vibration modes which are considered to be sensitive to resonant effects; g_h is the h^{th} modal gust factor

$$g_h = \sqrt{2\ln(f_h T)} + \frac{0.577}{\sqrt{2\ln(f_h T)}}, \tag{8}$$

f_h being the natural frequency of the h^{th} mode and T the sample length (typically one hour); σ^2_{Rh} the variance of response R associated to the mode h. The latter can be computed from modal analysis. Let $\psi_h(x,y)$ be the h^{th} mode shape, R_h the response corresponding to this deflection; $m(x,y)$ the mass per unit area; ξ_h the h^{th} modal damping. The h^{th} modal mass and load are:

$$M_h = \int_A m(x,y)\cdot\psi_h^2(x,y)\cdot dA; \qquad Q_h(t) = \int_A p(x,y,t)\cdot\psi_h(x,y)\cdot dA \tag{9}$$

Finally:

$$\sigma^2_{R_h} = R_h^2 \frac{\pi}{4\cdot\xi_h} \frac{f_h \cdot S_{Q_h}(f_h)}{(2\cdot\pi\cdot f_h)^4 M_h^2}, \tag{10}$$

$S_{Qh}(f)$ being the modal force spectrum. For the case study of Braga Stadium, 10 structural vibration modes have been considered. The damping ratio ξ_h = 0.01 has been assumed for all modes. The already cited Tab. 1 shows the strong influence of resonant effects in determining the global structural response.

2.6. Comments

The experimental data show the pressure coefficients to be significantly lower – both in mean values and standard deviation – than those reported by standards (EC1) for similar geometry. Large values are essentially confined to the roof borders, corresponding to local vortex shedding.

Table 1. Comparison of mean, quasi-steady and resonant contributions: vertical displacement, wind 270° from north.

Node	$\overline{R}$	$g^2_{qs}\sigma^2_{R,qs}$	$\overline{R} \pm \sqrt{g^2_{qs}\sigma^2_{R,qs}}$	$g^2_{res}\sigma^2_{R,res}$	$\overline{R} \pm \sqrt{g^2_{qs}\sigma^2_{R,qs} + g^2_{res}\sigma^2_{R,res}}$
A	0,1550	0,0250	0,3131	0,3027	0,7275
B	-0,0837	0,0115	-0,1910	0,3076	-0,6486
C	-0,0441	0,0014	-0,0812	0,0433	-0,2555
D	0,0930	0,0052	0,1652	0,0419	0,3101
E	0,0621	0,0092	0,1582	0,2040	0,5238
F	-0,0198	0,0016	-0,0599	0,2018	-0,4709

Hence, vortex induced pressures seem to not affect the global roof dynamics even if they can induce significant local stresses on the roof panels.
The POD has been used to simply evaluate the quasi-steady effects. The derived responses result lower than those derived by the standard (EC1) approach. Hence, the spatial uncorrelation effects should be greater than those approximately taken into account by the EC1 simplified procedures.
Very important resonant effects have been found. They are dominant in determining the peak responses for most of the wind directions. These effects are strictly related to the damping ratio which has been assumed to be 1% for all considered vibration modes: the monitoring system which has just been arranged on the real structure, seems to show values of ξ even smaller.

3. THE AEROELASTIC STUDY

The tests, carried out at the Politecnico di Milano BLWT, were performed on a 1:70 aeroelastic model of the Braga stadium in both laminar flow (without surrounding topography, to check the presence of possible forms of aeroelastic instabilities) and turbulent flow (with surrounding topography, in order to establish the response of the roof structure to the action of turbulent wind). Roof acceleration, displacement, strain and related mean drag forces were measured at different significant points. The following results were pointed out (see also Diana et al., 2003):

- The aeroelastic stability has been proved, up to 7m/s, corresponding to 58m/s in the full scale;
- The response to turbulent wind, with the effect of surrounding topography, showed, at the nominal design speed with 20% turbulence, amplitude levels that, at full scale, are of the order of 40÷50cm, with acceleration due to the first modes that reach peaks up to 1.5÷2m/s^2 and RMS values of 0.46m/s^2 A peak value of 2m/s^2 means that the overload due to dynamic motion is 20% of the dead load.
- The amplitudes of vibration generally found at the maximum speed are to be considered not acceptable, since there are uncertainties on the effective value of the turbulence on site and of the damping of the structure, which can cause a significant variation from the values found on the model. Therefore, in order to decrease such levels, and control their variation due to the parameters uncertainties (real damping and turbulence level), damping devices can be installed on the structure.
- In order to simulate their effect, proper dampers have been designed and implemented on the model, in order to increase the structural damping up to a maximum value of 7-8%. This allow to decrease the vibrations at 50% of the original global levels of vibration while the amplitude of the torsional frequency is reduced by a factor three, so showing the effectiveness of such devices. In the full scale, the required damping of each of the four dampers is in the range 100-l50kNs/m, i.e. as an ordinary ant-yaw dampers of train.

4. A SENSIBILITY ANALYSIS

This section presents a reliability analysis of the roof of the Stadium of Braga under random wind loads without consideration of the dynamic amplification due to the structural response. The extensive explanation of the problem can be found in Bertero et al., 2003. The following results are obtained: a) the sensibility of the failure probability of the roof to the spatial random distribution of wind loads, b) the wind direction that drive the structure to fail with most probability (considering all wind direction with a uniform distribution), c) the points of the roof that will fail with most probability, and d) the spatial distribution of wind loads that drive the structure to fail with most probability. Wind pressures are derived from the RWDI wind tunnel study. The roof was divided in 24 sectors (Fig. 1b) where the wind pressure where measured and averaged at any time t. Therefore, the wind loads on the roof are represented as randomly distributed pressures $\mathbf{X}$ in n (=24) sectors with mean values $\boldsymbol{\mu}$ and covariance matrix $\boldsymbol{C}$. In the analysis of the roof, the bending moments at m (=130) points will be considered.

4.1. The probabilistic model

A probabilistic model of the roof to random wind loads is analyzed classifying the data in deterministic and probabilistic as follows. Deterministic data are: n = Number of roof sectors = 24; m = Number of points on the plate to evaluate the reliability = 130; k = Number of the load case

considered acting simultaneously with the wind load = 1 = dead loads; $\mathbf{M_{Gx}}$, $\mathbf{M_{Gy}}$, $\mathbf{M_{Gxy}}$ = Bending and torsional moment vectors for load case k (rows = 130); $\mathbf{A_x}$, $\mathbf{A_y}$, $\mathbf{A_{xy}}$ = Matrix formed by the bending-torsional moments originated at each point of the plate by an unitary pressure in each sector (rows = 130, columns = 24); $\mathbf{M_{Upx}}$, $\mathbf{M_{Upy}}$, $\mathbf{M_{Unx}}$, $\mathbf{M_{Unx}}$ = Ultimate resistance positive-negative bending moments for each plate point (rows = 130).
For each wind direction the following probabilistic description was considered for the randomly distributed pressures $\boldsymbol{X}$ in the *n* sectors: $\boldsymbol{\mu}$ = Vector of mean values of $\boldsymbol{X}$; $\boldsymbol{C}$ = Covariance Matrix of the randomly distributed pressures $\boldsymbol{X}$; $\boldsymbol{f_X(X)}$ = Probability density function of the random variables**.** Correlated normal distribution with parameters $\boldsymbol{\mu}$ and $\boldsymbol{C}$.
Sets of correlated normal variables $\boldsymbol{X}$ can be simulated from sets of uncorrelated standard normal distribution variables $\boldsymbol{Z}$ by using the Cholesky decomposition of the correlation matrix $\boldsymbol{C}$, that is:

$$\mathbf{X} = \mathbf{L} \cdot \mathbf{Z} + \boldsymbol{\mu}_X , \qquad \mathbf{C} = \mathbf{L} \cdot \mathbf{L}^T , \tag{11}$$

L being an inner triangular matrix obtained by the Cholesky decomposition of **C** and **Z** is a vector of uncorrelated standard normal distributed variables. Lets assume that a wind pressure ΔX_j is simulated for each zone or the roof *j*. For each point of the slab, *i*, the bending and torsional moments, M_x, M_y and M_{xy} can be computed as follow:

$$M_{h,i} = M_{Gh,i} + \sum_{j=1}^{n} A_{h,ij} \cdot \Delta X_j , \qquad h = x,\ y,\ xy. \tag{12}$$

Considering the bending moments in each direction, the failure functions at each point of the plate ($1 \le r \le 130$), $G_r(\mathbf{X})$, are the following hyperplanes:

$$M_{Uph} - \left(M_{Gh,i} + \sum_{j=1}^{n} A_{h,ij} \cdot \Delta X_j \right) < 0 , \text{ and } M_{Unh} - Abs\left(M_{Gh,i} + \sum_{j=1}^{n} A_{h,ij} \cdot \Delta X_j \right) < 0 \tag{13}$$

where $G_r \le 0$ is failure and M_{Uxy} is computed from the Johanssen Theory as the smallest of $(M_{Upx}+M_{Upy})/2$ and $(M_{Unx}+M_{Uny})/2$. The failure condition is obtained when failure is reached at any point of the plate, i.e., the structural failure can be defined as $(G_1 \le 0) \cup (G_2 \le 0) \cup \ldots \cup (G_{130} \le 0)$. The failure probability is given by the probability that an outcome of the random variables $\boldsymbol{X}$ belongs to the failure domain, $\boldsymbol{D_f}$, defined by equations above. This probability is expressed by the following integral:

$$\int_{D_f} f_X(X) \cdot d(X). \tag{14}$$

The Orientated Simulation Method (Puppo and Bertero, 1992) was used to evaluate the probability of the Eq. (14).

4.2. Results

In order to identify the most dangerous wind direction, the minimum reliability index β for each direction was calculated. Fig. 4b summarizes the obtained index β for each direction. Therefore 300° is the wind direction that drives the structure to fail with most probability. Fig. 4a shows the distribution of β values along the slab. The zone with smallest values of β is related to the zone with maximum bending moment for the gravity load on the border where the wind load attack the roof.
Note that this method provides the worst spatial wind load distribution associated to the wind variability and the weakness of the roof. Therefore, at this purpose, this reliability-based method can be better than the POD, since in the POD method the obtained distribution depend only on the wind load variability itself. It was found that the spatial distribution of wind loads that drive the structure to fail with most probability is considerably different to that assumed in codes for design. However, the values are acceptable for static wind analysis.

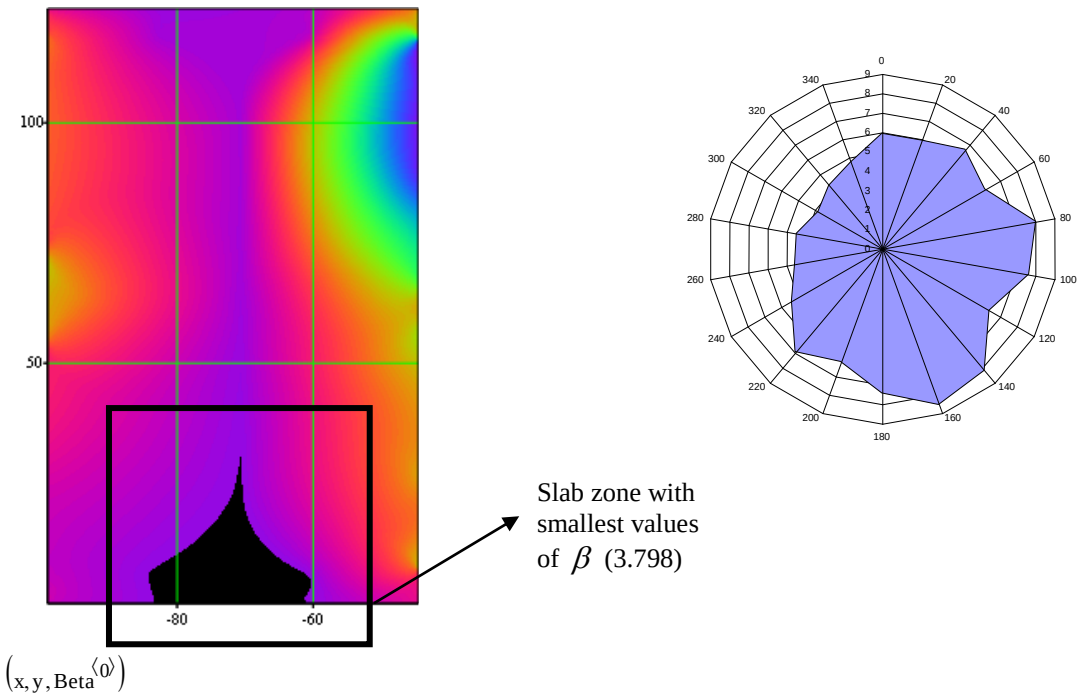

Figure 4. Mapping of the β values for wind direction of 300° (a) and minimun β value for different wind directions (b).

5. PRELIMINARY DESIGN OF AN ADDITIONAL DAMPING SYSTEM

The analysis of wind effects showed that the wind induced vibrations can reach very high amplitudes. Vibration amplitudes are very sensitive to the inherent structural damping ratio (approximately inversely proportional to $\sqrt{\xi}$). In those analysis a damping ratio of 1% was assumed for each natural vibration mode, but strong uncertainties characterize this value. Whenever the actual inherent damping will be lower than 1%, the wind induced vibrations could reach even larger amplitudes than the estimated ones. Hence, it seems important to monitor the actual structural damping. If it results insufficient to adequately contain the vibration amplitudes, it will be necessary to add a damping system which guaranties an acceptable level of wind induced oscillations. In the following, the main properties of such a damping system have been preliminary evaluated.

5.1. The dampers location

The presence of a stiff beam at the inner borders of the roof (from points B to F and A to E in Fig. 1b) induces the firsts natural modes, which are the most excited by the wind turbulence, to have the largest amplitudes at the ends of the beams themselves. Thus, the beam ends (points A, B, E and F) are among the most quoted to locate external dampers. These are also among the few locations compatible with the architectural requirements.

Hence, the analyzed damping system consists of four linear viscous dampers located at the inner vertices of the roof, C being the damping coefficients of dampers installed at points A, B, E and F. As a matter of fact, the dampers will be located at the ground level and connected to the roof by mean of tensile strands. Thus, a mass or a spring will be necessary to avoid compression in the cables. Nevertheless, in the present preliminary analysis the only presence of a simple linear viscous damper has been considered, without taking into account the added mass or stiffness, the mean value of the cable tensile force, etc.

A deeper stage of the design should evaluate the specific problems as, for instance, the opportunity to realize a friction damping system rather than a viscous one, the devices to avoid the cable slackening, the support induced cable excitation, etc.

5.2. Estimation of the added damping ratio through complex eigenvalue analysis

A preliminary estimation of the damping system efficiency has been carried out by mean of the eigenvalue analysis of the non-classical damped system. The eigenproblem is formulated by considering the firsts 10 modes of the undamped structure and the 4 added linear viscous dampers.

The firsts 4 complex modes have been analyzed (the higher ones requiring a more refined model). Fig. 5a shows the damping ratio associated to such modes, for different values of the damping coefficient. Additional damping ratio of 4% and more and a significant reduction of the oscillation amplitudes on the firsts non-classical modes can be achieved by using viscous dampers with a damping coefficient C=15000 kg_f s/m. Fig. 5b shows the real part of the 1st complex eigenvector.
In order to validate the analysis of the damping ratio, the time history analysis of free vibration induced by different impulses has been numerically carried out (modal superposition of the firsts 21 undamped modes). The modal identification has been made by the POD of the time series and the subsequent evaluation of the logarithmic decrement. The analyzed conditions substantially confirm the above evaluated damping ratio.

5.3. Effects of the damping system on the wind induced vibrations

In order to evaluate the realistic behavior of the damping system and the maximum force produced by the dampers, different time history analysis of the structure subjected to the pressure fields measured in the wind tunnel have been carried out. Tab. 2 shows a comparison of the structural responses (in terms of vertical displacements at the most significant points) in absence and with external dampers; the wind pressures were derived from RWDI wind tunnel tests, with the wind blowing from 270° to the true north. The velocity amplitude at the damper locations are also reported.
A significant reduction of the oscillation amplitudes (see standard deviations) can be obtained by using viscous dampers with a damping coefficient C=15000 kgf s/m. The subsequent damping force will reach an amplitude (derived from the value of $V_{max,damp}$ reported in Tab. 2) of about 6 tons, as order of magnitude.

6. CONCLUSIONS

In the present paper the characteristics of the unsteady wind pressures and their effects on the Braga Stadium suspended roof have been analyzed. The design wind speed has been conservatively assumed to be constant for all wind incidence, without taking into account for directionality effects. The experimental data show the pressure coefficients to be significantly lower – both in mean values and standard deviation – than those reported by standards (EC1) for similar geometry. Large values are essentially confined to the roof borders, corresponding to local vortex shedding. Hence, vortex induced pressures seem to not affect the global roof dynamics.
The proper orthogonal decomposition (POD) has been used to simply evaluate the quasi-steady effects. The derived quasi-steady responses result lower than those derived by the standard (EC1) approach.

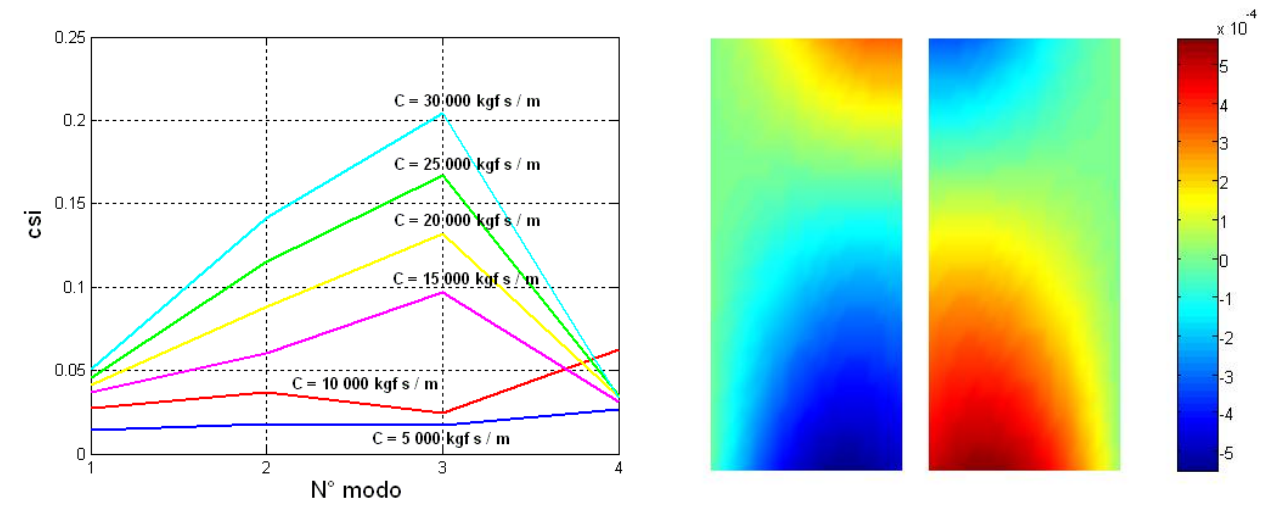

Figure 5. Damping ratio of complex modes (a) and real part of the 1st complex eigenvector - f_1=0,28 Hz - ξ_1=3,7% (b).

Table 2. Comparison of the structural responses (vertical displacements) in absence and with external dampers.

	ξ_i=1% - C=0 kg_f s/m				ξ_i=1% - C=15000 kg_f s/m				
	min [cm]	*max* [cm]	μ [cm]	σ [cm]	*min* [cm]	*max* [cm]	μ [cm]	σ [cm]	$V_{max,damp}$ [m/s]
A	-34	+32	+2	10,6	-11	+14	+2	3,8	≈0,27
B	-46	+39	-6	11,1	-24	+10	-6	4,9	≈0,37
E	-35	+48	+8	16,4	-13	+31	+8	6,0	≈0,41
F	-60	+26	-15	16,2	-38	+3	-15	6,8	≈0,34

Very important resonant effects have been found. They are dominant in determining the peak responses for most of the wind directions. It is important to observe that these effects are strictly related to the damping ratio (which has been assumed to be 1% for all considered vibration modes). On the other hand, the structural uncertainties – a complete monitoring system is working on the real structure and actual data will be available in the next future – do not allow to reliably assume larger values of ξ.

The large evaluated resonant effects suggested to study in depth the possibility to have exciting aeroelastic phenomena and to foresee, at the design stage, the possibility of introducing damping devices. At this purpose, an aeroelastic model of the roof was tested in the BLWT of Dept. of Mechanics of Politecnico in Milano. The aeroelastic stability was proved, up to 7m/s, corresponding to 58m/s in the full scale. On the other hand, the amplitudes of vibration generally found at the maximum speed are to be considered not acceptable, since there are uncertainties on the effective value of the turbulence on site and of the damping of the structure, which can cause a significant variation from the values found on the model.

Hence, the realization of an external damping system could be necessary. The analyzed (both theoretically and experimentally on the aeroelastic model) system consists of four linear viscous dampers located at the inner vertices of the roof. The analysis showed that an additional damping ratio of 4% and more and a significant reduction of the oscillation amplitudes on the firsts non-classical modes can be obtained by using viscous dampers with a damping coefficient C=150 kN s/m.

Finally, a sensibility analysis was carried out and it allowed to determine: the sensibility of the failure probability of the roof to the spatial random distribution of wind loads; the wind direction that drive the structure to fail with most probability , the points of the roof that will fail with most probability; the spatial distribution of wind loads that drive the structure to fail with most probability.

7. REFERENCES

Vickery, B.J., Wind loads on the Olympic Stadium: Orthogonal Decomposition and Dynamic (Resonant) Effects, *Report BLWT-SS28A*-1993.

RWDI, Wind tunnel study of roof wind pressures, Braga Stadium, *Report 01-327*, October 2001.

Ove Arup, Wind climate analysis report, Braga Stadium, *Report 66161*, September 2001.

Diana, G., Bocciolone, M., Collina, A., Tosi, A., Rocchi, D., Wind tunnel investigation on Braga Stadium. *Final Report*, February 2003.

Bertero, R.D., Carnicer, R., Puppo, A.H., Sensibility wind analysis of the roof structural system - Stadium of Braga - Portugal, *Final Report*, September 2003.

Puppo, A.H., Bertero, R.D., Evaluation of Probabilities using Orientated Simulation, *Journal of Structural Engineering, ASCE*, Vol. 118, No. 6, June 1992.